SESSION E—FEW-NUCLEON PROBLEMS

CHAIRMAN: *I. Slaus*

Experimental Investigations of Several Few-Nucleon Systems*

PAUL F. DONOVAN

Bell Telephone Laboratories, Inc., Murray Hill, New Jersey and Brookhaven National Laboratory, Upton, Long Island, New York

I. INTRODUCTION AND EXPERIMENTAL TECHNIQUE

In this article the most prominent and striking experimental features of reactions of few-nucleon systems producing three particles in the final state are presented and discussed. The use and usefulness of on-line computer and "data simulation" techniques is also described.

The experimental evidence which is presented indicates, at least in the case of few-nucleon systems, that reactions of the type $1+2\rightarrow 3+4+5$ proceed largely by one or both of two predominant mechanisms: either via the formation of an intermediate system, e.g., $1+2\rightarrow 3+(4, 5)^*\rightarrow 3+4+5$, or by the direct production via a knockout or exchange process of the three final-state particles. These two processes can, under suitable conditions, produce experimental phenomena which are surprisingly similar.

The formation of intermediate excited systems, or, which is kinematically equivalent, final-state interactions of relatively long duration, may be conveniently observed in reactions of the type $1+2\rightarrow 3+4+5$. The technique we have used is to measure the energies of two coincident emitted particles (by our convention particles 3 and 4), at angles θ_3 and θ_4; their kinetic energies are T_3 and T_4. A plot of T_3 versus T_4 yields a curve which is described by an equation of the 4th degree.[1] If the reaction proceeds in two steps, that is, if there are final-state interactions of long duration, then final-state interactions or intermediate energy levels will manifest themselves as regions of high density of events along such T_3 versus T_4 curves. The formation of a T_3 versus T_4 curve of the type described above constitutes a characteristic signature of a reaction producing three particles in the final state. A reaction producing only two particles in the final state will appear on a T_3 versus T_4 diagram as a spot, or at most as a pair of spots, and these spots will furthermore appear only at special angles of the two detectors, due to the conservation of momentum and energy. If, on the other hand, a reaction produces four or more bodies in the final state, and the energies of two are measured as described above, then the T_3 versus T_4 diagram yields not a curve but rather an area of events bounded by a curve. Any final-state interactions between two of the particles in a reaction producing four particles in the final state will then manifest themselves by the formation of three-body type curves in or bounding the allowed region for four-particle events.

There are a number of advantages in using reactions with 3 particles in the final state to study final-state interactions between the various particles. By measuring the energy correlations between two of the emitted particles, one can measure many final-state interactions in several systems in a single experiment. One gets the sort of information that could be obtained by studying the excitation functions of the scattering of the two relevant particles, and one is able to get this information with an accelerator of fixed beam energy. From an experimental point of view, one has the advantage of doing a coincidence experiment, with the attendent reduction of background, to gain information about a system which does not live long enough to reach the detector. In reactions involving light targets, the center-of-mass motion can be utilized as a kind of amplifier to provide very accurate measurements of the energies of any final-state interactions which are near the particle emission threshold. The use of this "amplifier" to provide a highly accurate measurement of the energy of the first excited state of He^4 is shown subsequently.

In our studies of few-nucleon systems the external particle beams of the Brookhaven National Laboratory

* This work was supported in part by the U. S. Atomic Energy Commission.

[1] For a more complete discussion of the kinematics of this type of reaction, see the preceding paper by Č. Zupančič, Rev. Mod. Phys. **37**, 330 (1965).

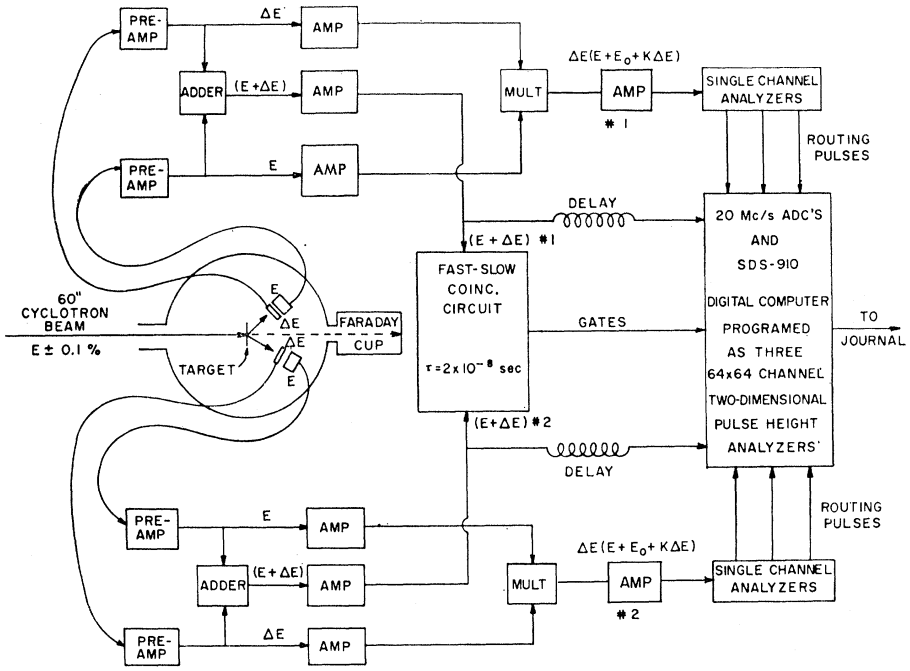

FIG. 1. A block diagram of the experimental apparatus.

60-in. cyclotron were used. These consist of $^1H_2^+$, $^2H^+$, $^3He^{++}$, and $^4He^{++}$ particles at energies of approximately 10 MeV per nucleon. They were momentum analyzed to $\pm 0.1\%$ and collimated to a 2-mm spot of negligible divergence. Under these conditions beam intensities of 10 to 100 nA were available.

Our experimental particle detection system consists of two semiconductor detector telescopes contained in a scattering chamber so constructed that the detectors can be moved independently to any pair of angles containing the beam axis in a common plane. A block diagram of the experimental setup is shown in Fig. 1. Each detector telescope contains two detectors; the first (labeled ΔE in Fig. 1) has a thickness of 15 to 100 μ and is used to measure the rate of energy loss (dE/dx) of a charged particle passing through it. The second detector (labeled E in Fig. 1) is a 3-mm-thick lithium-drifted silicon device which measures the residual energy (E) of the particle. The outputs of these two detectors, after suitable amplification, are fed into a pulse multiplier which provides an output of the form $\Delta E(E+E_0+K\Delta E)$, where E_0 and K are adjustable parameters. This output serves to identify the various particle types.

The preamplified signals from the ΔE and E detectors are also added to form a pulse whose height is proportional to the total particle energy. These pulses from both of the detector telescopes enter a fast–slow coincidence circuit with a fast resolving time of $\tau=2\times10^{-8}$ sec which gates on the analog-to-digital converters. Since the BNL cyclotron has an frequency of 11 Mc/sec this resolving time allowed us to resolve individual beam bursts. There are two ADC's, each with 4096 channels and operating at a clock frequency of 20 Mc/sec.

The device used for storage and display is a Scientific Data Systems model 910 general-purpose digital computer. The computer has been programmed to store and display three 64-x 64-channel arrays of data under the control of routing pulses from the particle identification system. If additional precision is needed in the energy measurement, each event may be recorded on magnetic tape as a pair of 12-bit addresses, so that each of the three areas may consist of an array of 16 777 216 channels.

The detailed kinematics of reactions producing three particles in the final state is quite complicated. If all three of the final-state particles are identical, a single energy level in an intermediate system can appear in up to twelve places along the kinematic curve. Often a given initial system can produce a variety of three-body reactions. For these reasons, the on-line computer is used to generate T_3 versus T_4 curves showing relevant kinematic and theoretical information presented in the same display format as the experimental data for rapid and accurate comparison during the experiment. Several examples illustrating the usefulness of this technique are seen shortly.

Although, in principle, the predictions of theory may be compared with experimental data in any relevant coordinate system, the most common procedure is to transform the experimental data into the coordinate system in which the theory assumes its simplest mathematical form. Although this method seems straightforward and attractive, especially to theoreticians, it

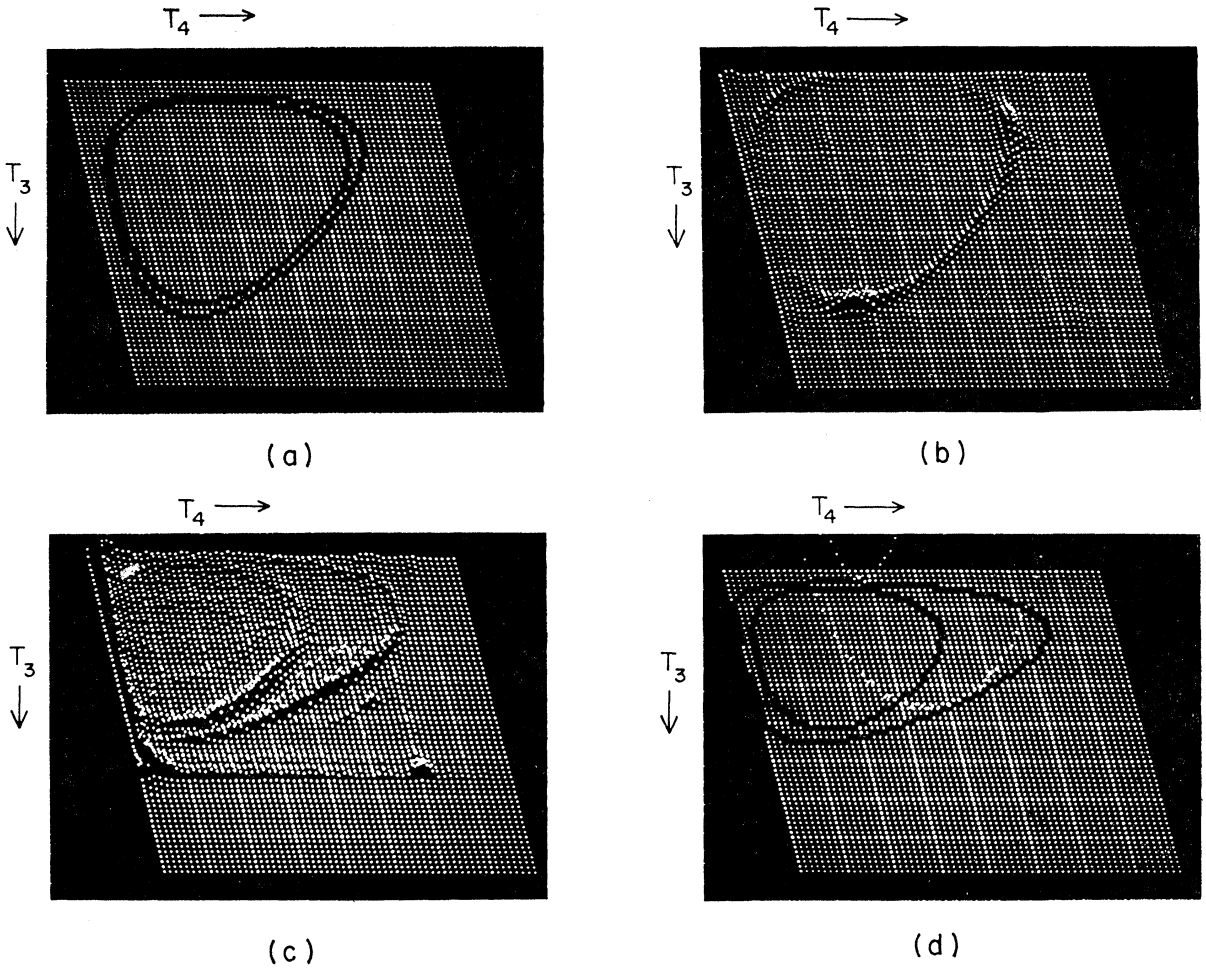

FIG. 2. Experimental data and computer-generated kinematic curves for the reactions $d+p\rightarrow p+p+n$ and $d+d\rightarrow d+p+n$.

does have disadvantages when the transformations involved are sufficiently severe to change greatly the appearance of the experimental data. The principle disadvantage is that one loses sight of the sensitivity of the comparison of theory with experiment, to the actual laboratory parameters which are after all the only means one has of changing experimental conditions. Since one of the principle advantages of an on-line computer system is (or should be) the enhancement of the experimenter's ability to recognize during the experiment any novel or unexpected features of the data, malfunctions of the apparatus, etc., we have evolved the above mentioned procedure of performing at least our intial comparison of the experiment with the predictions of kinematics and theory, in the laboratory system. We refer to this technique as "data simulation." Another advantage of this method is that it avoids the necessity of performing time-consuming on-line transformations of each experimental event. Such transformations are complicated by the effects of target thickness and by the fact that the finite angular resolution of the detector telescopes leads to ambiguities in the selection of angles for the coordinate transformation of any particular channel from the T_3, T_4 space. In general, the data simulation technique has proven its great utility in a wide variety of experimental investigations.

II. FINAL-STATE INTERACTIONS AND SPECTATOR POLES: THE REACTIONS $D+P\rightarrow P+P+N$ AND $D+D\rightarrow D+P+N$

The reaction $d+p\rightarrow p+p+n$ was investigated by directing the well-analyzed and collimated cyclotron beam of 21.1-MeV deuterons onto a thin polyethylene target. $p-p$ coincidences were measured using the technique described above. The kinematically predicted curve in (T_3, T_4) space for the angles $\theta_3=26°$, $\theta_4=-26°$ (opposite sides of the beam axis) is shown by the computer generated curves in Fig. 2(a). The photographs in Fig. 2 were made directly from the

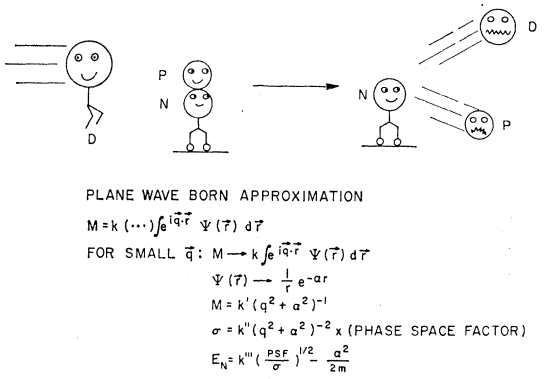

FIG. 3. A plane-wave knockout model for the reaction $d+d\rightarrow d+p+n$. **q** is the laboratory momentum of the spectator neutron **r** is the relative distance coordinate in the deuteron target, Ψ is the deuteron wave function, α is the characteristic relative internal momentum in the deuteron, m is the reduced mass, E_n the laboratory neutron kinetic energy, σ the reaction cross section, and PSF means phase-space factor.

cathode-ray-tube display generated by the computer. The area between the two curves is due to the angular spread of the detectors, which was $\pm 1.25°$. The energy calibration is 12 MeV in T_3(ch48) and T_4(ch48). The corresponding experimental data are shown in the "curve" display of Fig. 2(b). In this form of display, regions of high cross section manifest themselves by upward displacement of the grid points. The two pronounced bumps at the outer extremes of the experimental curve occur in the regions of very low energy (about 100 keV) in the two possible intermediate $(p+n)$ systems, and are due to the formation of singlet $(T=1)$ deuterons. Although the width of these peaks is perhaps 100 keV in the $(p+n)$ systems, their laboratory width is about 2 MeV; such amplification effects are due to the center-of-mass motion, and in this case we are thus able to obtain data on the p–n final state interaction in an energy region which is not conveniently accessible to direct scattering measurements.

In Fig. 2(b), a broad peak is seen in the region of low T_3 and T_4, which corresponds to an excitation in the $(p+p)$ system of about 850 keV. We believe this peak is not an effect of the p–p final-state interaction, but rather is attributable to a direct knockout effect of a type which is discussed shortly. Besides the three pronounced peaks seen in Fig. 2(b), there is a region of high intensity between the two singlet deuteron peaks. This intense ridge may be the result of the increased phase space available in this region of the curve, or it may also be a direct knockout effect.

In order to examine a three-body-breakup reaction in which there were no strong resonances expected, the reaction $d+d\rightarrow d+p+n$ was investigated, using as a target a thin deuterated polythylene foil. No strong peaks were expected in the experimental data, since there are no known sharp resonances in the possible intermediate systems $(d+p)$ and $(d+n)$, and the formation of the singlet deuteron is forbidden by isospin conservation since it is $T=1$ and all the other particles are $T=0$. The experimental data for the angles $\theta_3=24°$, $\theta_4=-46.3°$ are shown in Fig. 2(c). The energy calibration is 10 MeV in T_3(ch48) and T_4(ch24). Since the two charged particles detected in the final state of the reaction are of different masses, there are two p–d coincidence curves. It was not neccessary to separate them by particle identification since they do not overlap in the energy regions of interest. There is also a faint closed curve nearer to the origin which is attributed to the reaction $d+p\rightarrow p+p+n$ from the hydrogen impurity in the deuterated polyethylene target. Several straight lines and spots due to random coincidences and two-body reactions are also visible. The outer p–d coincidence curve, which is formed by the deuteron going to θ_3 and the proton to θ_4, has a very strong peak which is seen as a faint broad curve of white dots above the black part of the data curve. Measurements at many angles have shown that this peak is not a final-state interaction in any possible intermediate system, although it cannot be distinguished from such by a measurement at a single pair of angles; rather, it always appears when the laboratory momentum of the unobserved neutron is very small. Although this peak is several MeV broad in the T_3 or T_4 coordinate, it is much sharper in the laboratory neutron energy, which we call T_5. At this pair of angles most of the reaction cross section appears in a region where T_5 is less than about 200 keV. Figure 2(d) shows the computer-generated kinematic curves calculated for the detector angular centers. The curved lines of white dots are raised above the black kinematic lines by an amount proportional to T_5. It is seen that in the region of the experimental peak, T_5 rapidly approaches zero. The small curve of white dots in the upper part of Fig. 2(d) has been raised from the high T_3 region of the inner p–d coincidence curve, thus showing that T_5 does not approach zero along this curve. The strong peaking at low values of T_5 is a general feature of the various reactions we have investigated. We attribute these

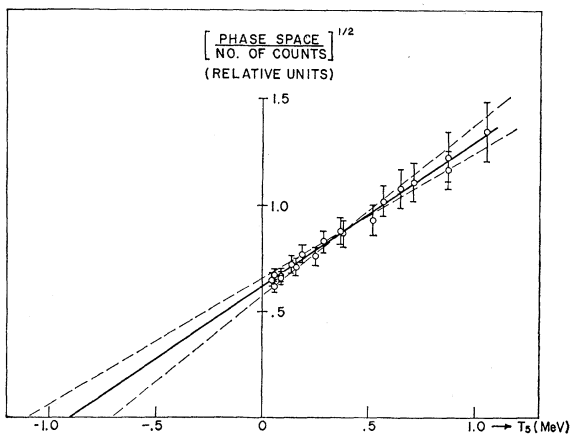

FIG. 4. A Chew–Low plot of the data of Fig. 26.

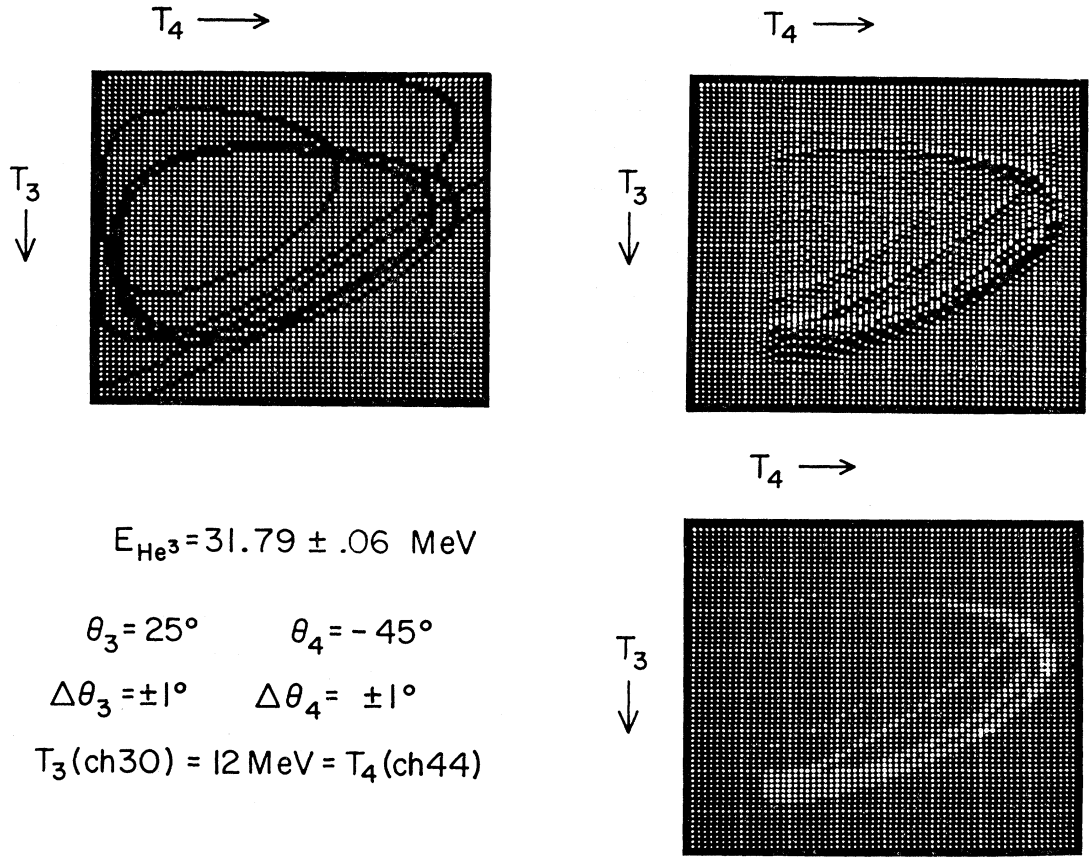

FIG. 5. Data and kinematic predictions for reactions of He^3+d and He^3+C^{12}.

"giant" peaks to the tendency for a direct knockout process to form spectator particles. A simple plane-wave, hard-sphere knockout calculation of this process is outlined in Fig. 3. We consider the projectile deuteron to be an elementary particle, and the target deuteron to be a bound state of a proton with the neutron.[2] In the matrix element, the effect of small neutron momentum is expressed by a term of the type shown in Fig. 3. We assume that in the region of small neutron momentum this term varies much more rapidly than any other term in the matrix element, and hence all other terms are taken to be constant. For the case of small momentum transfer to the neutron in the target, it becomes accurate to use the asymptotic form of the deuteron bound-state wave-function as shown in Fig. 3. We see from the expression for the form of the cross section that if the square root of the quotient of the phase space divided by the cross section per T_3 channel is plotted versus T_5, the laboratory kinetic energy of the spectator neutron, a straight line should be obtained intersecting the T_5 axis at a negative (unphysical) energy of $-\alpha^2/2m$. In this case the intercept is just half the deuteron binding energy or -1.1 MeV. The results of such a plot for the data of Fig. 2(c) are shown in Fig. 4. We see that within the experimental error this very simple theory appears to describe accurately the giant peak in the data. Of course, since in this reaction we have two identical particles in the initial state, we certainly should expect another giant peak of the same sort, the second arising from the case where no momentum is transferred to the neutron contained in the projectile instead of that in the target. There should, as well, be two more peaks arising from the cases of low momentum transfer to the protons of both the projectile and the target. These latter two peaks would be more difficult to observe experimentally, since in the case of low momentum transfer to the proton in the target we would have to detect a very low energy proton, and in the case of low momentum transfer to the proton of the projectile we would expect this proton to proceed to nearly 0° in the laboratory system. These spectator poles have been observed in a variety of reactions and are quite easy to confuse with final-state interactions or resonances in some intermediate system, unless one takes great care in the measurement of their position as a function of the angles of the detectors. The region of low T_5 in the $d+p \rightarrow p+p+n$ reaction shown in Fig. 2(b) is distributed over a very broad region of the T_3 versus T_4 data curve, and so this spec-

[2] See the preceding paper by Č. Zupančič (Ref. 1) for a more complete theory of this process.

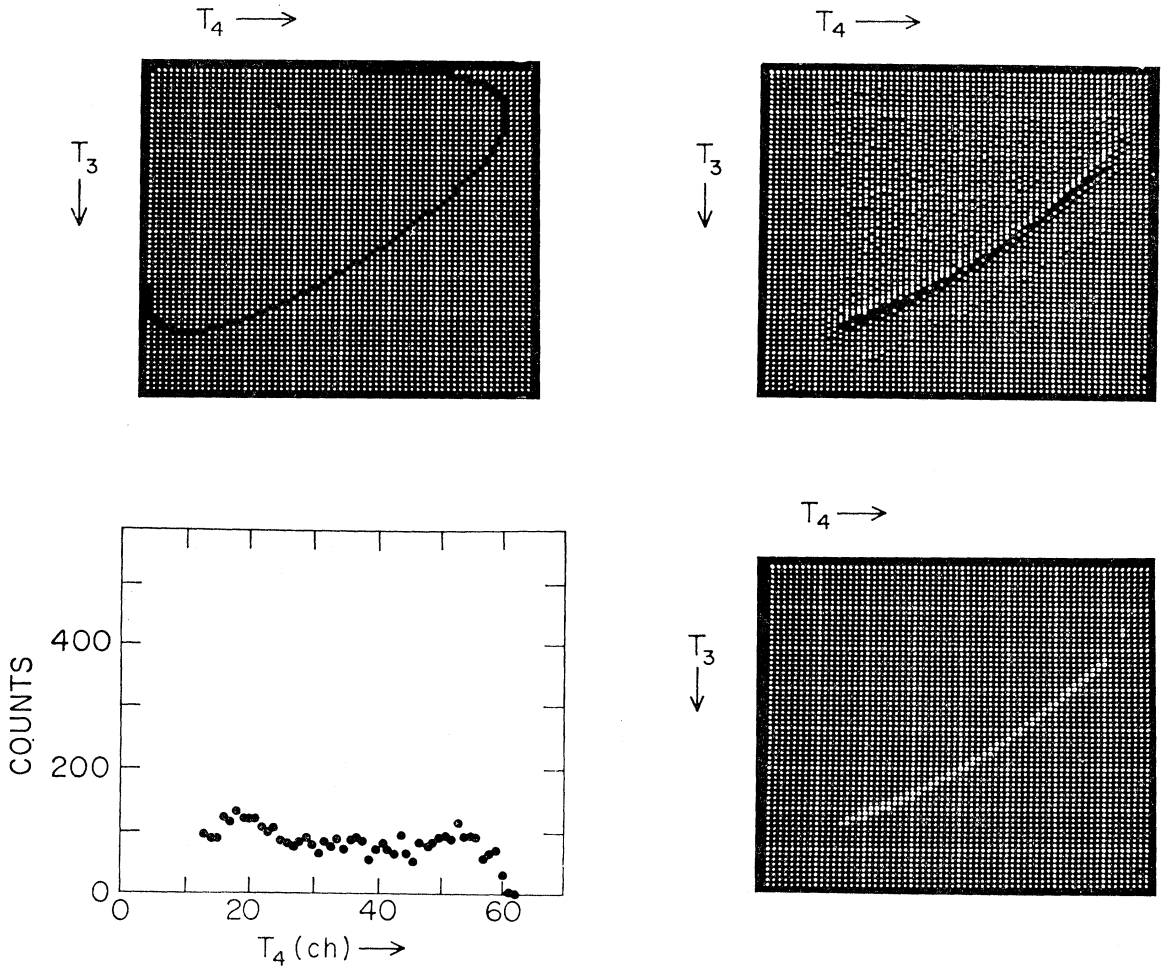

FIG. 6. Data and kinematic predictions for p–p coincidences from the reaction $He^3+d\rightarrow p+p+t$.

tator process may contribute to a large extent in the intensely populated region along that curve between the singlet deuteron peaks. In this reaction, the effect of low momentum transfer to the neutron of the projectile deuteron also contributes to the intensity of the curve in the region of the peak at the low T_3 and T_4 coordinates. In any case, the appearance of such strong poles in the experimental data acquired in a variety of reactions is certainly worthy of further experimental and theoretical investigation.

III. THE LEVEL STRUCTURE OF He^4

In recent years, increased attention has been given to the search for energy levels in He^4. We have used the reaction $He^3+d\rightarrow p+He^{4*}$ to look for coincidences between protons populating energy levels of He^4, and breakup particles from the decay of these levels. In addition to the usual reduction of background achieved in coincidence experiments, this technique has the advantage of identifying the mode of decay of any observed energy levels. Also, as will be seen, the energies of the particles emitted in the decay of a level located near the emission threshold provide a particularly sensitive measure of the energy of that level, relative to the threshold energy.

The magnetically analyzed 31.8-MeV He^3 beam of the Brookhaven National Laboratory 60-in. cyclotron was collimated to a 2-mm-diam spot and directed onto a deuterium target made of a thin deuterated polyethylene foil. The experimental technique involved in the detection and measurement of charged particles emitted from the target was as described in Sec. I.

There are three possible three-particle-breakup reactions of the $(d+He^3)$ system at our energy, any of which may proceed via energy levels in He^4: they are $He^3+d\rightarrow p+p+t$, $He^3+d\rightarrow p+n+He^3$, and $He^3+d\rightarrow p+d+d$. The target contains C^{12}, so the reactions $He^3+C^{12}\rightarrow p+d+C^{12}$ and $He^3+C^{12}\rightarrow p+p+C^{13}$ are also seen. Since there are many possible combinations of coincident charged particles in these reactions, the use of the computer during the course of the experiments to

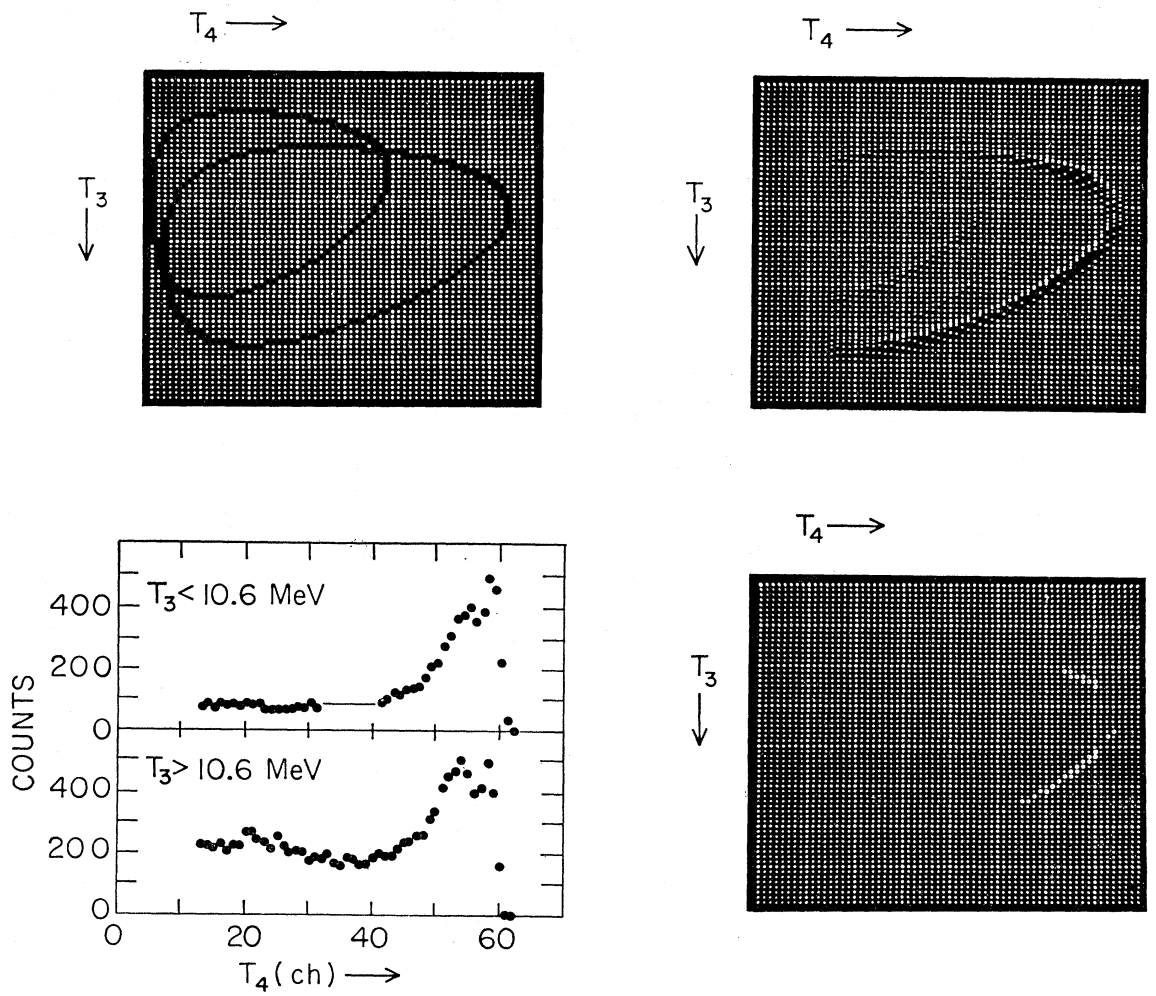

FIG. 7. Data and kinematic predictions for p–p and p–d coincidences from the reactions $He^3+d\rightarrow t+p+p$ and $He^3+d\rightarrow d+p+d$.

generate a kinematic prediction of the form of the incoming data, as described previously, was particularly useful.

Figure 5 shows the kinematic predictions and experimental data under the indicated experimental conditions as they would appear if the various reactions were not further separated by particle identification. (These experimental data were actually obtained by summing the three computer display areas). Figure 5 and several subsequent figures contain photographs of "map" as well as "curve"-type computer CRT displays. The "map" photographs may be taken at various threshold settings, the brightly illuminated channels containing numbers of events in excess of the threshold setting. The data curves are somewhat smeared due to the effects of target thickness and finite angular aperture.

If the reactions of the (He^3+d) system proceed in two steps involving excited states of the He^4 nucleus, e.g., $He^3+d\rightarrow p+He^{4*}\rightarrow p+p+t$, then there will be associated intensity maxima at the appropriate proton energies on the coincidence curves. At the angles shown in Fig. 5, ($\theta_3=25°$, $\theta_4=-45°$) the charged particle on the T_4 axis must be a proton because calculation shows that the associated d, t, or He^3 cannot reach as large an angle as 45°. Therefore, for the purpose of particle separation at these angles, a proton channel was set on the T_4 axis, and proton, deuteron plus triton, and He^3 channels were set on the T_3 axis to route to sections 1, 2, and 3 of the computer display area, respectively. The finite thickness of the ΔE detector unfortunately leads to a low-energy cutoff which is particularly severe on the T_3 axis when the relatively short-range He^3 particles are involved, but the advantages of the particle identification easily outweigh the disadvantages of this effect, particularly in the case of the p–t and p–He^3 coincidence curves, which otherwise are nearly juxtaposed.

Figure 6 shows the calculated curve and the data from display area 1 ($p-p$ coincidences). The calculated line is for $p-p$ coincidences from the reaction $He^3+d\rightarrow p+p+t$. In the "curve" picture of the data a faint line is seen at high energies from the reaction $He^3+C^{12}\rightarrow$

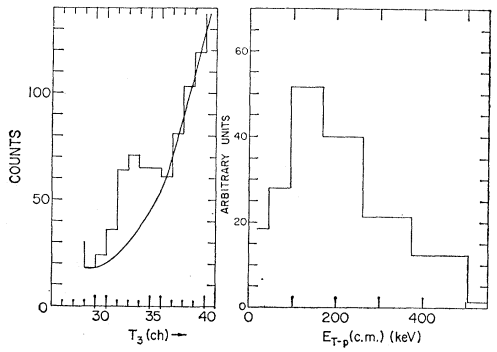

FIG. 8. The first excited state of He^4. Left side: A projection onto the T_3 axis of a region of the p–t coincidence curve of Fig. 7. Right side: These projected data with an estimated continuum subtracted. The ordinate is the number of counts per unit energy in the $(t+p)$ system, in relative units, and the abcissa is the energy in the $(t+p)$ system.

$p+p+C^{13}$. The "map" picture of the data does not show much structure, although there is some indication of a slight peak at T_4(ch59). A more quantitative measure of the structure along the $p-p$ curve is seen in the graph of Fig. 6 which shows a projection of the line onto the T_4 axis. No pronounced structure is observed, although there is some evidence for a broad peak centered aroung T_4(ch53).

Figure 7 shows the data from display area 2 (protons on the T_4 axis, deuterons and tritons on the T_3 axis) together with the relevant calculated curves from the He^3+d reactions. The $p-d$ coincidence curve is seen to be very weak. The strongest curve is due to $p-t$ coincidences from the reaction $He^3+d\rightarrow t+p+p$. There is another faint line noticeable in the curve picture, which is formed by $p-d$ coincidences from the reaction $He^3+C^{12}\rightarrow d+p+C^{12}$. Considerable structure is seen along the $p-t$ line in both the curve and map pictures. The graph, which shows the projection of the $p-t$ line, has been broken into two sections because of the double-valued nature of the coincidence line. The principle features seen in the projection are a narrow peak at T_4(ch58) and a broader peak centered at about T_4(ch53.5). These two peaks have been repeatedly measured at many angles and are observed to be well-behaved energy levels of He^4 in the sense that their energies and widths in the He^4 center-of-mass system are independent of the angles of observation.

A very accurate determination of the energy of the sharp (first-excited state) peak in the He^4 system can be made because of the "kinematic amplifier" effect. Since this state gives rise to a pair of peaks appearing on the coincidence line in a region where it is nearly parallel to the T_3 axis, the triton energy (T_3) provides a much more sensitive measure of the position of the level relative to the threshold energy than does the energy (T_4) of the proton emitted in forming the state. This is illustrated by projecting one of these peaks from the data of Fig. 7 onto the T_3 axis. This projection is shown in the left half of Fig. 8. After subtracting an estimate of the contribution of the higher excited state and continuum as shown in the figure, the number of counts per unit ϵ as a function of ϵ may be calculated. (ϵ is the He^4 excitation energy minus the $p-t$ threshold energy). This is shown in the right half of Fig. 8. The result of such graphs calculated from data taken at many pairs of angles have been summed and are shown in Fig. 9. This result gives the energy of the first excited state of He^4 as 19.94 ± 0.02 MeV, with a width of about 100 keV, which is an accuracy much greater than we could obtain with our apparatus by measuring the proton energy.

Figure 10 shows the data and calculations relevant to display area 3. (proton on the T_4 axis and He^3 on the T_3 axis). The data are cut off below about T_3(ch20) because of the thickness of the ΔE detector, so that only the high T_3 wing of the normally double-valued curve is seen. The intense line is due to the $He^3+d\rightarrow He^3+p+n$ reaction and shows the second excited state of He^4 appearing strongly. The first excited state cannot appear on this line since it lies below the (He^3+n) threshold. There is another strong, broad peak in the vicinity of T_4(ch16). This is seen best in the projection onto the T_4 axis shown in Fig. 10 and is caused by the formation of singlet ($T=1$) deuterons. The energy in the $(p+n)$ system becomes low in this region of the coincidence curve. The absence of a corresponding peak in the projection of the $p-t$ coincidence curve of Fig. 7 indicates that there is essentially no tendency to form a diproton system. This conclusion was also arrived at on theoretical grounds in the preceding lecture by Zupančič. The projection of Fig. 10 shows another interesting feature, which is the strong "tail" on the second excited state peak in the region T_4(ch40–50). This is actually a knockout pole of the type discussed previously, forming

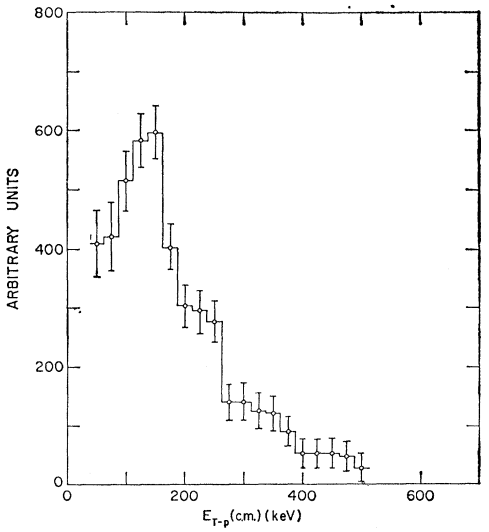

FIG. 9. The first excited state of He^4. A sum of projected data taken at many pairs of angles, in the form of the plot in the right side of Fig. 8.

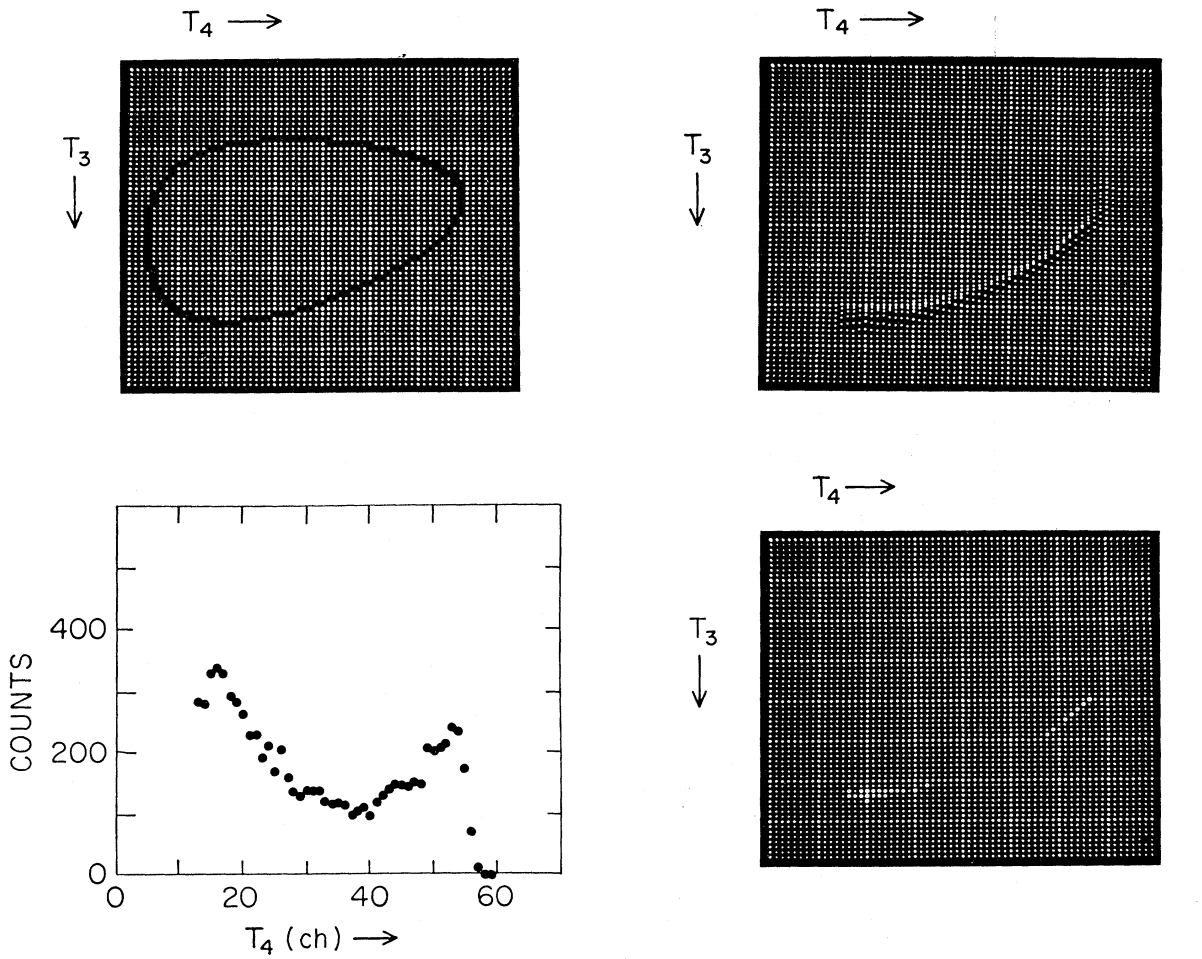

FIG. 10. Data and kinematic predictions for p–He^3 coincidences from the reaction $He^3+d \rightarrow He^3+p+n$.

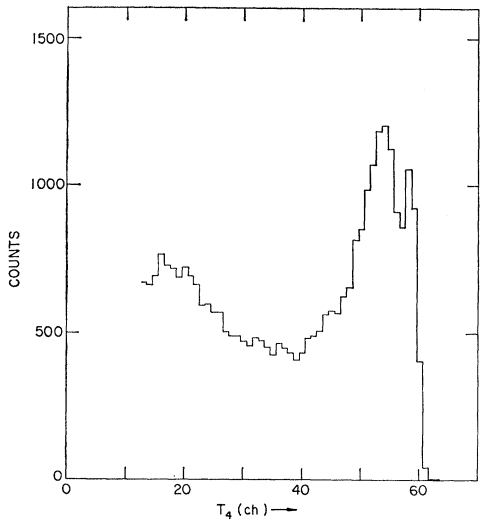

FIG. 11. A summed projection onto the T_4 axis of the p–p, p–t, and p–He^3 coincidence lines of Figs. 6, 7, and 10, showing both excited states of He^4.

spectator neutrons from the deuteron target. At some angles this pole is more intense than the He^4 excited states which occur nearby, and hence one can see that it is of the utmost importance that poles be properly identified and not confused with energy levels.

Figure 11 shows a sum of the projections of Figs. 6, 7, and 10. An average of such data taken at many pairs of angles gives the energy of the second excited state of He^4 as 21.24 ± 0.20 MeV, with a width of about 1.2 MeV. An energy-level diagram of He^4 based on these data is shown in Fig. 12.

In conclusion, it should be pointed out that one of the most serious and time-consuming problems in experiments of this type is the problem of data handling all of which has so far been done by hand. Our most recent advance in the use of the computer to help us with future data reduction involves the use of a light pen to indicate areas of particular interest along the coincidence curves by simply touching the light pen to the desired regions on the cathode-ray-tube oscilloscope when the map form of display is being used. The light-pen-indicated areas are erased from the display and the

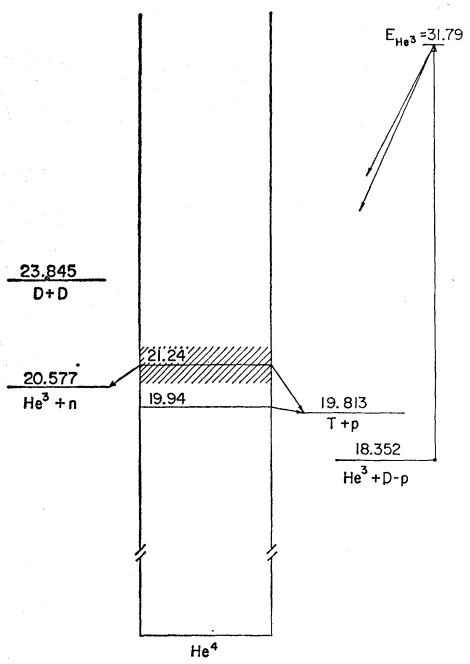

FIG. 12. Energy-level diagram for He^4.

corresponding channel numbers and counts therein contained are stored in the computer. After typing into the computer the various identifying characteristics of the reaction which has just been indicated, the computer then transforms these data into any desired set of coordinates, such as excitation energy in some intermediate system, and then displays the results in the form of a histogram with the appropriate scale numbers appearing along the axes. This procedure enables us to avoid the tedious process of looking at all of the numbers which we have recorded, and makes full use of the ability of the experimenter to solve pattern recognition problems by eye which be very difficult indeed for a computer to do. While in the most refined final treatment of the data one would wish to make appropriate background corrections and corrections for target thickness, etc., nevertheless the availability of such a program enables us to examine the data in the system of the greatest theoretical interest quickly and easily during the course of the experiment.

ACKNOWLEDGMENTS

The work reported here is the result of a group effort. The participants, besides myself, are P. D. Parker of Brookhaven National Laboratory, and J. V. Kane, J. F. Mollenauer, and Č. Zupančič, all of Bell Telephone Laboratories and Brookhaven National Laboratory.

Discussion

KRAMER: I would like to hear about your explanation of the broad structures which you see in this reaction. You made some explanation for the peak, but I did not quite understand what your explanation was for the broad structures.

DONOVAN: You mean the places where there are no peaks?

KRAMER: The places where there are few events; a smooth curve, and you don't have the peaks.

DONOVAN: Yes. Those are all nonresonant processes. You can, if you like, consider them to be the tails of very broad, high-lying states, whose centers are very far removed from the energy region of interest. You can always treat it formally that way. Of course, we don't know the details—in fact, there aren't any prominent details, as you can see from the data.

KAMKE: Did you try to plot a complete Dalitz plot, so it shows not only two angles or one angle? In changing the angle you get a complete picture of the reaction.

DONOVAN: No. We didn't try to do that. As you are well aware, you can't do that. Let us estimate, even with 64-channel resolution, the number of events which are required to get statistics sufficient to prepare pictures like the ones I have shown in every region of the Dalitz diagram. You have all those pairs of coplanar angles and then have to go out of the plane as well, so that even if you only wanted a few counts per channel, you would need over a billion events. Therefore, you really can't hope to do the complete job. So you have to do something else.

Well, what are you going to do? What we have done is to try to figure out where the prominent features of the data lie, based, for example, on the sequential process, or on some kind of direct knockout process, and to pick out particular regions of the Dalitz diagram, which diagram ordinarily integrates over all the angles. We keep those regions separated so we can keep track of the angular correlations. We select for investigation the regions which are most sensitive to the particular phenomena we are trying to investigate; and our data simulation technique tells us where to look.

Since we can't do everything, we want to make sure every event we do measure is most sensitive to the processes we are looking for. So that's what we do.

ZUPANČIČ: I would just like to point out that there is nothing ideal about the Dalitz plot. In a reaction where you have two particles coming in and three going out, as I said and everybody knows, we have, apart from the incident energy, four independent variables. So if you really want it to be perfect, you would have to make a four-dimensional Dalitz plot.

Now this is possible in the sense you can introduce invariant variables such as to give the plot simple boundaries and a constant phase-space density, but it is in four dimensions. So the only thing you could do is to store it in the memory of a large computer and make two-dimensional sections through it, and look at it.

Now as soon as you decide, at the beginning, on the two coordinates which you are going to pick out, you prejudice yourself in the sense that you assume a particular mechanism to take place. So this is fine if you know beforehand what you are going to look for; what kind of a mechanism you are going to expect. But then there is nothing very general about it any more. You might as well proceed in the way in which Donovan indicated; namely, you take your expected theory and transform it into the laboratory system.

O'CONNELL: What is the explanation in the $D+p$ for the bump that used to be the diproton?

DONOVAN: I'm sorry. I never did get to that, did I? This is in the region of one of the knockout poles. If the neutron of the projectile deuteron is a spectator, it continues on at a high energy at an angle near zero degrees. This condition obtains in a region which is quite close—not exactly on top of, but quite close, to the peak at low T_3, T_4 in Fig. 2(b).

We have seen this peak persist at other angles where the relative

energy in the p–p system is up around 2 MeV or more. You certainly don't expect to see a diproton at that energy, but we still do see this peak in the experimental data; hence it is probably a manifestation of that pole. On the other hand I must caution you, we haven't done quantitative analyses of those data. We merely know that the observed peak is close to where the pole is predicted.

O'CONNELL: The Chew–Low plot you did do should come out half the binding energy of the deuteron. Are you satisfied it is close enough to that?

DONOVAN: It is certainly within the limits of our experimental data. I think our data line, where it intersected the negative energy axis is a bit below 1 MeV. The two other lines represent an eye-ball estimate of the error.

ALBURGER: Is there anything you can say about the theoretical interpretation of the two He^4 levels?

DONOVAN: No; not really. It is quite difficult, knowing only the energies. We have not measured any information yet about the spins and parities. That is the next project. We now want to look at the angular correlation of the decay particles; this should enable us to extract angular momentum.

I want to point out that the case where we knock a deuteron apart is not the only case where we have observed a strong knock-out pole. Recently we did a measurement with 40-MeV alphas on Li^6 to produce alpha+alpha+D. Here again practically the entire cross section was contained in a peak which was near the region of the Chew–Low pole. This phenomenon is not just a characteristic of the deuteron wave function, but I am sure it is something which will be seen time and again.

HOLMGREN: Do you see any four-body breakup in your D+D experiment?

DONOVAN: Yes.

HOLMGREN: If so, how much goes by the four-body compared with the three-body?

DONOVAN: Well, you see it is rather difficult for us to say. I can certainly tell you that at all the angles we have investigated the answer is not very much. Just perhaps a few percent, or so.

On the other hand, you have to remember that a direct process like the formation of that spectator neutron peak that we see involves events that are nearly coplanar with the beam axis, for the simple reason that, since the neutron carries very little momentum, the other two particles have to be coplanar by conservation of momentum.

If we examined noncoplanar events, we might find that the situation is reversed. Since we haven't done that, I would not care to guess what the relative intensities of these two processes are.

PUGH: How do your results on $^6Li(\alpha, 2\alpha)$ compare with the results we heard earlier on $^6Li(p, pd)$? We had a number of results on the momentum transfer distribution.

DONOVAN: Yes. I would like to make two remarks. First of all, you can either knock out the deuteron or the alpha particle, leaving the other as a spectator. We chose to knock out the deuteron for the reason that it then is possible to get closer in the physical region to the pole. This just comes out of the kinematics. So it is really not quite a direct comparison.

All I can say is that we have not yet Chew–Low plotted these data because we don't have statistics yet that we are satisfied with.

But we have noticed that it is not going to work quite as the deuteron case because the peaks in the experimental data do not come exactly at the minimum T_5. One expects more severe distortions with alphas on ^6Li; the Coulomb force is more important, and one will need a more sophisticated treatment than the one we could get away with for deuterons on deuterons.